Hydration of Isobutene in Liquid-full and Trickle-bed Reactors

Rates of hydration of isobutene were measured with Amberlyst-15 catalyst particles in a differential, liquid-full recycle reactor operating at atmospheric pressure and 303 to 333 K. Catalysts pretreated in two different ways were studied. Liquid-to-particle mass transfer had a small but measurable effect on the rate. Intraparticle diffusion was more significant, as indicated by effectiveness factors from 0.26 for the larger catalyst particles ($d_p = 1.04 \times 10^{-3}$ m) at 333 K to 0.84 for the smaller particles ($d_p = 0.45 \times 10^{-3}$ m) at 303 K. The intrinsic rate was first-order in isobutene concentration with an activation energy of 67 kJ/mol. The intraparticle diffusion resistance is due to the macropores surrounding the very small gel-type microparticles of which the particles were composed.

Some data were obtained for reaction rates in trickle-bed operation. Global rates were somewhat lower in the trickle-bed operation than in the liquid-full runs. Using the previously determined intrinsic kinetics and effectiveness factors, the liquid-to-particle mass transfer coefficients could be approximated for the trickle-bed operation.

Pak Leung, C. Zorrilla, F. Recasens, J. M. Smith
University of California
Davis, CA 95616

Introduction

Acidic ion-exchange resins catalyze the production of alcohols by hydration of the corresponding olefin (Kaiser et al., 1962; Neier and Woellner, 1973; Dooley et al., 1982). High equilibrium conversions are favored at low temperatures. The hydration of isobutene is of special interest because the product, tert-butyl alcohol (TBA), is useful as an octane improver, thus reducing the need for lead-based additives (O'Sullivan, 1985).

A key feature for a successful liquid-phase process is the method of overcoming the low solubility of isobutene in water. Some existing processes use either a cosolvent or a high TBA recycle stream to achieve complete miscibility. Trickle-bed operations (feed streams of liquid water and gaseous isobutene) may have economic advantages over using cosolvents or a series of slurry reactors with recycle. Operation at lower pressures is possible. Also, in trickle beds the high water concentration at the catalyst sites would shift the equilibrium conversion in the favorable direction. The low isobutene concentration in water would reduce by-product formation by dimerization. A disadvantage is the low rate of reaction at the low isobutene concentrations in the liquid phase. Also, high mass transfer rates from gas to liquid would be necessary in order to achieve high rates of reaction.

To evaluate the trickle-bed process, it is desirable to know the intrinsic kinetics at the catalyst sites, intraparticle diffusion within the resin beads, and the several interphase mass transport effects. A macroporous sulfonic acid catalyst such as Amberlyst-15 beads is preferred over gel-type resins. This is because of higher diffusion rates in the rigid macroporous matrix, in comparison with those in the gel structure (Kun and Kunin, 1967; Pitochelli, 1975). Liquid-phase diffusivities are so low that intraparticle diffusion often significantly retards the global rate. Hence, a primary objective of our work was to evaluate intrinsic kinetics and effectiveness factors for isobutene hydration using Amberlyst-15 beads. For this work a liquid-full (no gas phase) recycle reactor was used. A second objective was to obtain some rates of reaction in trickle-bed operation using pure isobutene gas and water saturated with isobutene as the feed streams. With data obtained in the two types of reactors, the mass transfer limitation in trickle-bed operation could be estimated. Concentrations of water were so large that nearly isothermal conditions prevailed.

To our knowledge intrinsic kinetics and effectiveness factors for isobutene hydration using macroporous Amberlyst-15 beads have not been published, nor is there information on reaction

The current address of C. Zorrilla and F. Recasens is Department of Chemical Engineering, Universitat Politecnica de Catalunya, Diagonal 647, 08028 Barcelona, Spain.

rates in trickle beds. Gupta and Douglas (1967) determined the first-order rate constant and intraparticle diffusivity for Dowex-50, a gel-type resin. The results suggested that surface migration in the gel structure contributed significantly to the global rate. The reverse reaction, dehyration of TBA, has been studied with both gel and macroporous ion-exchange catalysts (Heath and Gates, 1972; Gates and Rodriguez, 1973). These studies investigated the role of water in competition with TBA for the SO_3H active sites. Micro- and macropore diffusion has been studied with Amberlyst 15 beads (Ihn and Oh, 1984) for sucrose inversion.

In the temperature range of our work, 303–333 K, the hydration reaction is essentially irreversible. The measured equilibrium constant for this exothermic reaction is 40 at the higher temperature of 373 K. Prior papers (Lucas and Eberz, 1934; Kaiser et al., 1962; Gupta and Douglas, 1967) report first-order kinetics for olefin hydration in an excess of water. We have experimentally verified this conclusion.

While intrinsic kinetics and mass transfer limitations were not separated, Kaiser et al. (1962) measured conversions in an integral reactor of Amberlyst-15 particles for hydration of propylene. The results were interpreted in terms of first-order kinetics in olefin up to 40% conversion. An overall activation energy declined with temperature increase, suggesting that intraparticle and/or interphase mass transfer effects were significant.

Our liquid-full and trickle-bed reactors were operated with low conversions per pass ($\leq$10%) so that reaction rates could be obtained directly from the measurements of flow rate of liquid and TBA concentrations. The liquid was recycled through a saturator reservoir so that the feed water was always saturated with pure isobutene.

In order to check reproducibility of catalyst activity, two methods of pretreatment of Amberlyst-15 were used.

Experimental

Trickle-bed runs were made in the apparatus shown in Figure 1. The key items are the reactor *7* and the saturator reservoir *5*, which could be operated at different temperatures with separate constant-temperature baths *6*. Liquid saturated with isobutene was recycled downflow through the reactor. In this way the same concentration of isobutene was fed throughout the run. The cocurrent gas stream of pure isobutene passed once through the reactor. The pressure drop through the reactor was not negligible and varied with flow rate and temperature. Therefore, the reservoir and reactor were operated at slightly different temperatures so as to maintain an isobutene concentration in the liquid feed in equilibrium with the gas feed stream. Since the isobutene feed concentrations were constant and the conversion per pass was $\leq$10%, the reaction rate was constant during the time of a run, about 10.8 ks. The TBA concentration in the liquid was measured by taking samples at intervals from location *3*. This concentration accumulated to about 1.0 mol/m^3. This level was large enough for accurate measurement but not so large as to affect isobutene solubility or make the reverse reaction significant. The reservoir operated at essentially atmospheric pressure and the excess isobutene from it flowed through condenser *8*.

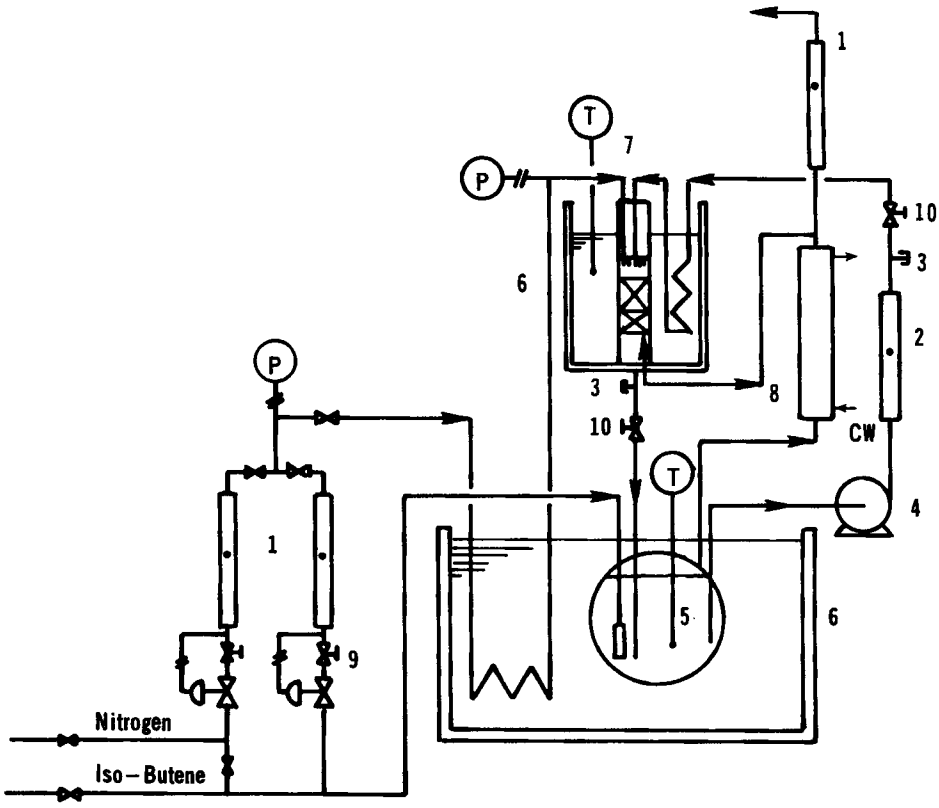

Figure 1. Apparatus.

1. Gas rotameters 2. Liquid rotameter 3. Sampling septa 4. Recycle pump 5. Reservoir with isobutene sparger 6. Constant-temperature baths 7. Trickle-bed reactor 8. Reflux condenser 9. Flow controllers 10. Needle valves

The condenser was to suppress water and TBA carryover from the reservoir. The recycle lines were insulated.

The trickle-bed reactor was a 1.5×10^{-2} m glass tube 0.3 m long. Liquid was fed through 12 (1.0×10^{-3} m ID, 5×10^{-3} m long) stainless steel capillary tubes located uniformly across the reactor cross-sectional area. A uniform height of liquid above the plate holding the tubes helped achieve equal flow in each capillary. The outlet of the tubes was 5×10^{-3} m above the prepacking of 0.45×10^{-3} m glass beads used to ensure further a uniform flow of liquid across the catalyst bed. Prepacking and catalyst bed, whose dimensions are given in Table 1, were supported by a stainless steel screen. The catalyst particle-to-tube diameter ratio satisfied the requirement for uniform liquid distribution according to the criterion of Herskowitz and Smith (1978).

For liquid-full runs the liquid flowed upward through a 1.2×10^{-2} m ID stainless steel tube. The catalyst bed was held between two stainless steel screens. Runs were made at four temperatures and for two sizes of catalyst particles, as shown in Table 1. In liquid-full experiments isobutene gas was fed only to the reservoir, and reservoir and reactor were operated at the same temperature. Operating conditions for both trickle-bed and liquid-full operation are given in Table 1.

Catalyst

Two types of Amberlyst-15, one initially wet (A-15W), and one dry (A-15D), were studied in order to test reproducibility and pretreatment. Intrinsic kinetics and intraparticle diffusivities were obtained for both types from liquid-full runs at different flow rates, particle sizes, and temperatures. Properties of the catalysts are given in Table 2. Chemically, they are sulfonated copolymers of styrene cross-linked with 20% divinylbenzene. Physically, the nearly spherical beads are agglomerates of gel-type microparticles estimated to be about 0.1 μm dia. (Dooley et al., 1982). Fragmentary information (Ihn and Oh, 1984) suggests that about 5% of the active SO_3H groups are on the outer surface of the microparticles and the remainder inside these small particles.

Table 1. Operating Conditions

Liquid-Full Reactor		
Catalyst particle size, $d_p \times 10^3$, m	0.45*	1.04*
Dry mass of catalyst, m $\times 10^3$, kg	1.90† and 1.95**	1.94† and 1.96**
Liquid flow rate, $Q_L \times 10^6$, m^3/s	2.1 to 9.25	
Temperature, K	303, 313, 323, 333	
Pressure at reservoir	Atmospheric	
Liquid volume in reservoir and lines, m^3	10^{-3}	
Flow rate of isobutene to reservoir, m^3/s	4.2×10^{-6}	
Trickle-Bed Reactor		
Catalyst and prepacking size, $d_p \times 10^3$, m	0.45	
Mass of catalyst, m $\times 10^3$, kg	0.778	
Glass bead prepacking height, m $\times 10^3$	13	
Catalyst height, m $\times 10^3$	10	
Liquid flow rate, m^3/s	0.55 to 3.42 $\times 10^{-6}$	
Gas flow rate, m^3/s	1.7 and 5.5 $\times 10^{-6}$	
Reactor temp., K	323	
Reactor gauge pressure, kPa	1 to 6	
Liquid volume in reservoir and lines, m^3	10^{-3}	

*Effective wet size, after conditioning dry-sieved fractions (35–50 and 18–20 mesh, resp.)
**Amberlyst-15 wet (A-15W) catalyst
†Amberlyst-15 (A-15D) catalyst

Table 2. Properties of Amberlyst-15*

	Grade	
	15 Dry	15 Wet
Type	Strongly acidic, cation exchanger	
Functional group	$-SO_3^- H^+$	$-SO_3^- H^+$
Physical Form	Beads	Beads
Max. operating temp.	394K	394K
Moisture content, as received	Less than 1%	50–55%
Surface area, m^2/kg	50×10^3	50×10^3
Porosity	0.36	0.36
Ion-exchange capacity, meq/g dry	4.7	4.7
Average pore dia.	24nm	—
Pellet size, 85% within	16–30 mesh	—

*Data from Rohm and Haas Co.

A single batch of dry catalyst was first sieved, retaining the 35-to-50 and 18-to-20 mesh ranges. The pretreatment for this catalyst consisted of mixing 20 to 50×10^{-3} kg amounts of a sieved fraction with 500×10^{-6} m^3 of distilled water and boiling with reflux for 14.4 ks. The mixture was then filtered under low vacuum so as not to remove intrapore water. A weighed amount of activated catalyst was then added to the reactor. Separately, a weighed amount of catalyst was dried in an oven at 393 K for 14 ks and weighed. Also, a sample of about 50 particles of the wet catalyst was examined microscopically to determine a number-average particle diameter. These experiments established both the weight of catalyst, on a dry basis, in the reactor and the wet-catalyst particle size.

The initially wet catalyst as received contained about 50 wt. % water. A single batch was first dried at 373 K for 14.4 ks and then sieved to give average particle sizes of 0.45 and 1.04×10^{-3} m (Table 1), as before. After boiling in distilled water, the dry weight and wet particle size were determined as described for the initially dry catalyst. Samples were then placed in the reactor and activated (as recommended by the manufacturer) by downflow of a 10 wt. % H_2SO_4 solution through the bed at a space velocity of 1.1×10^{-3} s^{-1}, until 1.5 bed volumes of solution had been used. Finally, the bed was rinsed with distilled water until the pH of the effluent was the same as that of distilled water. This acid pretreatment increased the reaction rate about 34%, indicating that the wet material, as received, could have contained some residue (soap, monomer, salts, etc.).

The pore-volume distribution of the dry catalyst was measured in a 60,000 psi (413.4 MPa) Aminco Porosimeter which permitted volumes to be measured down to 30Å (3 nm). Figure 2 shows the cumulative pore volume curve and the density, pore volume, porosity, and other particle properties calculated from the porosimeter data. The porosity and average pore diameter compare well with the information in Table 2 provided by the manufacturer. Figure 2 shows that about 75% of the pore vol-

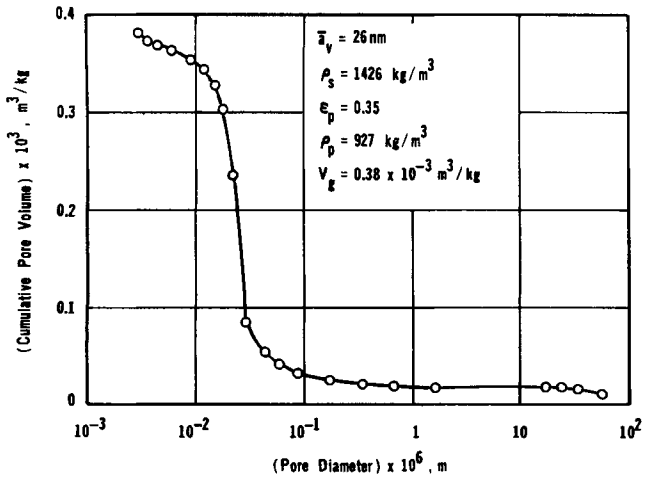

Figure 2. Cumulative pore volume vs. pore diameter for A-15D catalyst.

ume is in pores smaller than 30 nm. Presumably most of this 75% is due to microparticle porosity.

Chemicals

Isobutene, stated purity 99 mol %, from Phillips Chemical Co., was used without further purification. Tert-butyl alcohol and isopropyl alcohol, for chromatographic calibrations, were reagent grade, ACS certified, from Mallinkcrodt Chemical Co. Deionized plus distilled water was used.

Analytical procedure

Reaction rates were determined by analyzing samples of the recycle liquid for TBA using isopropyl alcohol as an internal standard. Since only 1×10^{-6} m^3 samples were needed, the total volume withdrawn from the batch liquid during a run was negligible (about 6×10^{-6} m^3 vs. a system volume of 10^{-3} m^3). Nitrogen was used as a carrier gas in the chromatograph, which was equipped with a flame-ionization detector and a column packed with 15% Carbowax 20 M on 80/100 mesh Chromosorb W and operated at 358 K.

Intrinsic Kinetics and Intraparticle Diffusion: Liquid-full Results

Figure 3 shows typical experimental data plotted as TBA concentration vs. time at 323 K for two flow rates and two particle sizes of the initially dry catalyst. The isobutene concentration in the feed liquid did not vary with time. The data points establish straight lines, showing that the rate is constant during a run. This indicates that the TBA concentration never reaches a high enough value to affect significantly the isobutene solubility in the reservoir or to cause a measurable amount of reverse reaction. The data for runs 79 and 80 at the same conditions agree well; the estimated difference in slope of the lines was 0.6%. Replicate runs separated by three months of catalyst use gave slopes within 2% of each other, suggesting little catalyst deactivation. Comparison of data for runs 80, 112, and 113 shows that there is a significant effect of catalyst particle size and a small effect of flow rate, Q_L.

Calculation of reaction rates

Because of its volatility a small amount of TBA was stripped from the reservoir by the isobutene gas stream. Not all of the alcohol was returned to the reservoir by the condenser. Hence, the calculation of the reaction rate required consideration of the TBA lost in the isobutene gas stream leaving the reservoir. This could be accounted for by writing the following mass balance of TBA over the entire system:

$$V_T\left(\frac{dC_A}{dt}\right) = mr - \begin{pmatrix}\text{rate of}\\ \text{TBA loss}\end{pmatrix} = mr - \alpha(C_A H_A) \qquad (1)$$

The last term assumes that the rate of loss of TBA (in the gas leaving the condenser) is proportional to TBA concentration, $C_A H_A$, in the gas leaving the reservoir. The isobutene gas rate bubbled through the reservoir was constant. Integrating Eq. 1 over the time of a run with $C_A(t = 0) = 0$, and solving for the constant rate, yields

$$r = \frac{C_A H_A \alpha}{m\left[1 - \exp\left(-\frac{\alpha H_A t}{V_T}\right)\right]} \qquad (2)$$

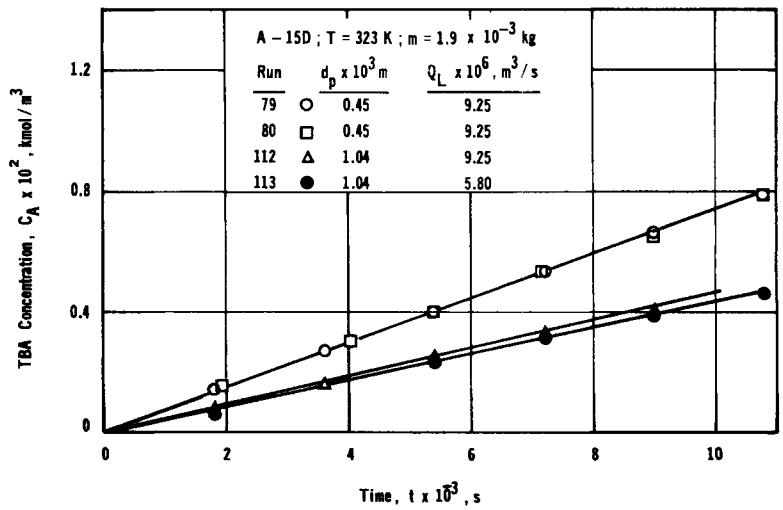

Figure 3. Accumulation of TBA vs. time in liquid-full recycle reactor for A-15D catalyst.

To establish the proportionality constant α, blank runs were made with the same flow rate of isobutene bubbled through the reservoir. In these runs, the reactor was bypassed and TBA added initially to the liquid so that Eq. 1 with $mr = 0$ is applicable. Analysis of the liquid concentration at intervals gave the evaporation rate and α. The value of α was not a function of the liquid recycle rate but varied with temperature. The ratio of evaporation rate to accumulation rate of TBA was 0.016, 0.033, 0.073, and 0.152 at 303, 313, 323, and 333 K, respectively. Hence the correction for evaporation was small.

Rates of reaction were calculated from Eq. 2 using the concentration vs. time curves such as shown in Figure 3.

Reaction order

To test reaction order, recycle liquid of different isobutene concentrations was obtained by bubbling different mixtures of helium and isobutene through the reservoir. Reaction rates were then calculated from Eq. 2. Rates were determined at high liquid rates and extrapolated to infinite flow rate (method described later) to eliminate the small amount of liquid-to-particle mass transfer resistance. Data for Henry's constant H for isobutene (Taft et al., 1955; Kazanskii, 1959) were used to calculate the isobutene concentration, C_L. Runs at 323 K using initially dry catalyst particles ($d_p = 0.45 \times 10^{-3}$ m) are shown in Figure 4. The straight line established by the data indicates the rate to be first-order in isobutene. While the rates include intraparticle diffusion retardation, for a first-order reaction the effectiveness factor is independent of concentration and does not affect the decision about reaction order, unless diffusion controls the rate ($\phi \geq 5$). For our conditions, the Thiele modulus was of the order of 1.0.

Rate measurements with TBA added to the liquid show, Table 3, that a sevenfold increase in TBA concentration reduced the rate by only 4%. The highest concentration, 2×10^{-2} kmol/m^3, is higher than the alcohol concentration at the termination of any of the runs.

Kinetics and intraparticle diffusion results

The first-order rate constants, k, and effectiveness factors, η, at 303 to 333 K were evaluated by determining reaction rates

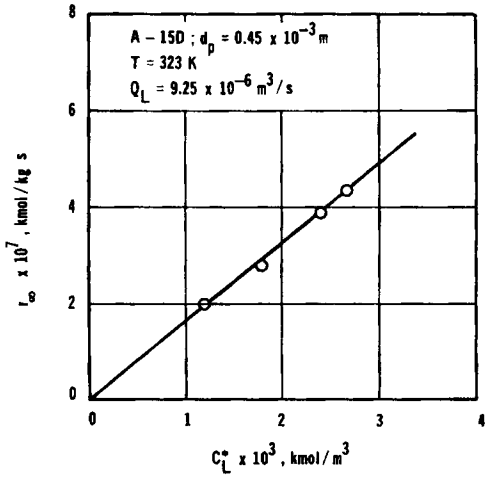

Figure 4. Effect of isobutene concentration on observed rate at highest liquid flow rate (liquid-full data).

Table 3. Effect of TBA on Reaction Rate at 323 K

C_{A_0} kmol/m^3	r kmol/s · kg dry catalyst
3×10^{-3}	4.17×10^{-7}
2×10^{-2}	4.00×10^{-7}

from Eq. 2 for various flow rates and for two sizes of catalyst particles. All these results were obtained from liquid-full data.

For a first-order reaction, k, η, and the liquid-to-particle mass transfer coefficient $(k_{Ls}a_s)_{Lf}$ are related by the equation

$$r = (k_{Ls}a_s)_{Lf}(C_L - C_s) = k\eta\, C_s \tag{3}$$

For differential reactor operation, the isobutene concentration in the liquid may be taken as the average of feed and effluent values, or

$$C_L = \frac{1}{2}\left[C_L^* + \left(C_L^* - \frac{rm}{Q_L}\right)\right] = C_L^* - \frac{rm}{2\,Q_L} \tag{4}$$

where C_L^* is the concentration in the liquid in equilibrium with pure isobutene gas and rm/Q_L is the difference between feed and effluent concentrations. Eliminating C_L and C_s from Eqs. 3 and 4 yields

$$\frac{C_L^*}{r} - \frac{m}{2\,Q_L} = \frac{1}{k\eta} + \frac{1}{(k_{Ls}a_s)_{Lf}} \tag{5}$$

Since $k\eta$ is independent of liquid flow rate, extrapolation of a plot of the lefthand side of Eq. 5 to infinite $(k_{Ls}a_s)_{Lf}$, or flow rate, yields $k\eta$. The correlation of Dwivedi and Upadhyay (1977) proposes that $k_{Ls}a_s$ is proportional to $Q_L^{0.59}$. We found that plotting $(C_L^*/r - m/2\,Q_L)$ vs. $Q_L^{-0.59}$ gave straight lines that could be extrapolated accurately to given $k\eta$. Figure 5 shows

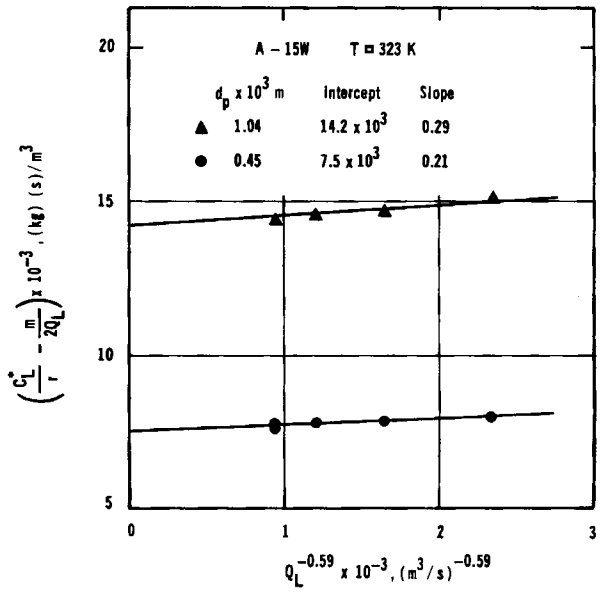

Figure 5. Effect of liquid flow rate (external diffusion) on global reaction rate for liquid-full operation at 323 K.

such lines for the two sizes of initially wet catalyst at 323 K. The small slopes of these lines in comparison with the intercepts show that liquid-to-particle mass transfer did not have much effect on the observed rate. Hence, $k\eta$ values could be evaluated accurately by this procedure but not $k_{Ls}a_s$. Nevertheless, $(k_{Ls}a_s)_{Lf}$ calculated from the slopes of the lines agreed within 30 to 50% of the Dwivedi and Upadhyay correlation. In Figure 5 the slope of line for the $d_p = 1.04 \times 10^{-3}$ m particles is somewhat larger than that for the smaller particles, as expected from the effect of particle size on $k_{Ls}a_s$.

The values of $k\eta$ for the two particle sizes at each temperature were determined by similar extrapolation to infinite flow rate. The results for both catalysts are given in Table 4. In these cases measurements at only one, high flow rate were made. Then the slope of the line was determined from the viscosity, diffusivity, and density at each temperature and the correlation of Dwivedi and Upadhyay. In terms of flow rate, the correlation may be expressed as

$$\frac{1}{k_{Ls}a_s} = K\left(\frac{\mu_L}{\rho_L D}\right)^{0.67}\left(\frac{d_p\rho_L}{\mu_L}\right)^{0.41}(Q_L)^{-0.59} \qquad (6)$$

where K is independent of temperature. Table 5 shows the physical properties and the solubility C_L^* of isobutene in water. The fourth column of Table 4 shows the resultant $k\eta$ values for all the data.

The $k\eta$ values, at the same temperature, for two particle sizes are sufficient to evaluate k and η (and D_e) separately, provided the η is not so low as to be in the asymptotic range where $\eta = 1/\phi$ (Smith, 1981). A further requirement is that the activity and porosity be the same for the two particle sizes, which is probably a good assumption since the two sizes were obtained by sieving the same batch of catalyst. The results for k, η, and the effective diffusivity are given in Table 4 for both catalysts.

As expected, η decreases with increasing temperature, and decreases with increasing particle size, with the decrease greater at higher temperatures. Intrinsic rate constants are nearly the same for the two catalysts. This is shown more clearly on the Arrhenius plot in Figure 6, which suggets an average activation energy of 67 kJ/mol. For the gel-type catalyst Gupta and Douglas (1967) found E to be about 100 kJ/mol. Effective diffusivities are given in the last column of Table 4. Values for this very sensitive quantity, which are of the expected magnitude for diffusion in liquid-filled pores, deviate between catalysts. Comparison of D_e with the bulk diffusivity of isobutene in water (D in Table 5) shows that D_e increases more rapidly with temperature, and ranges from 20 to 70% of D.

The effective diffusivity values are based upon a monodisperse pore-volume distribution, yet the data in Figure 2 show that the catalyst has a bidisperse pore structure. Figure 2 is in agreement with the description that the particles consist of an agglomerate of microspheres containing macropore volume between microparticles. Suppose that the microparticles have a diameter of about 0.1 to 0.2 $\times 10^{-6}$ m and that the micropore diffusivity within the gel-type particles is about 10% of the molecular diffusivity, as suggested by Satterfield (1970). Then the Thiele modulus for the microparticles is of the order of 10^{-3}, indicating an effectiveness factor of unity. Using the diffusivity for the gel-type Dowex-50 from Gupta and Douglas gives the same result. Accordingly, the diffusivities in Table 5 would refer to the inert macropore region. Ihn and Oh (1984) proposed that

Table 4. Intrinsic Kinetics for Isobutene Hydration on Amberlyst-15*

$d_p \times 10^{+3}$ m	T K	$k\eta \times 10^5$ m³/s · kg	η	ϕ	$k \times 10^5$ m³/s · kg	$D_e \times 10^{10}$ m²/s
		A-15 Dry Catalyst				
0.45	303	3.56	0.84	0.60	4.26	6.3
	313	8.35	0.77	0.77	11.0	9.6
	323	16.56	0.75	0.78	21.9	19.
	333	32.33	0.72	0.87	44.7	31.
1.04	303	2.35	0.55	1.37	4.26	6.3
	313	5.02	0.46	1.78	11.0	9.6
	323	9.89	0.45	1.80	21.9	19.
	333	18.67	0.42	1.99	44.7	31.
		A-15 Wet Catalyst				
0.45	303	3.14	0.78	0.73	4.02	3.7
	313	6.62	0.69	0.95	9.61	5.1
	323	13.32	0.62	1.15	21.5	8.0
	333	25.98	0.52	1.51	50.4	11.
1.04	303	1.93	0.48	1.67	4.02	3.7
	313	3.71	0.38	2.20	9.61	5.1
	323	7.10	0.33	2.65	21.5	8.0
	333	13.09	0.26	3.48	50.4	11.

*From liquid-full reactor studies.

Table 5. Isobutene Solubility in Water and Liquid Properties

	Temperture, K			
	303	313	323	333
$C_L^* \times 10^3$, kmol/m³*	4.66	3.55	2.68	1.93
$D \times 10^9$, m²/s**	2.12	2.7	3.29	3.98
$\mu_L \times 10^4$, kg/s · m	7.97	6.53	5.47	4.66
Sc	378	239	164	116
ρ_L, kg/m³	995	992	988	983

*From Kazanskii et al. (1959), at 100 kPa totl pressure (including water vapor).
**From Gehlawat and Sharma (1968) at 298 K, corrected for temperature according to Wilke-Chang dependence.

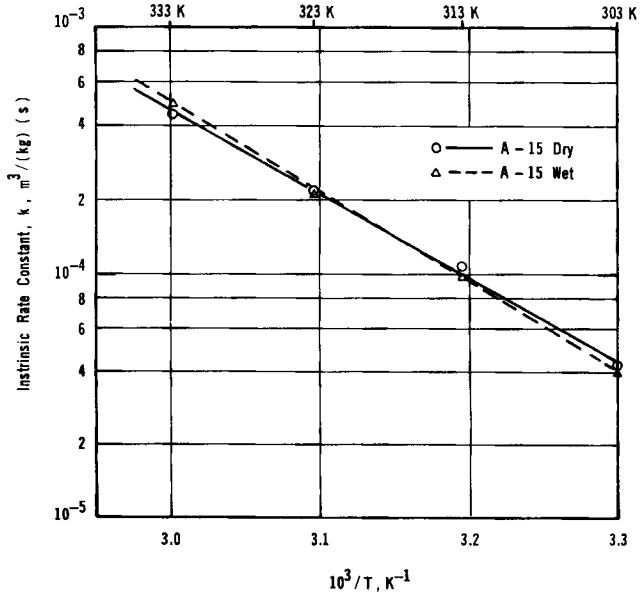

Figure 6. Arrhenius plot of first-order rate constant.

nearly all (95%) of the active SO_3H groups were within the microparticles.

Gupta and Douglas found that the effective diffusivity in their gel-type catalyst decreased with temperature, suggesting surface migration in the gel. In contrast, the diffusivities for Amberlyst-15 increase with temperature (Table 5). This supplements the conclusion that the D_e values in Table 5 refer to the macropore region rather than to the gel structure within the microparticles.

Trickle-bed Results

In trickle beds at low liquid flow rates only part of the outer particle surface is covered with rivulets of flowing liquid. Small interparticle spaces can be occupied by nearly stagnant liquid and other parts of the surface may be separated from the gas by only a thin layer of liquid. Despite its unrealistic simplicity, it has become customary to consider the surface to be covered either with flowing rivulets or with a thin layer of liquid, the latter termed the "gas-covered" surface (Satterfield, 1975). The wetting efficiency is defined as the fraction of the surface covered by flowing liquid.

As the liquid rate increases the wetting efficiency approaches 100% (Satterfield, 1975; Herskowitz et al., 1979; Morita and Smith, 1978). For these conditions with a reactant only in the gas phase, reaction occurs by mass transfer from gas to liquid, then transport from liquid to outer surface of the particle followed by intraparticle diffusion and reaction. If the gas and liquid feed streams are in equilibrium with respect to the gaseous reactant (isobutene in our case), and if this equilibrium is maintained in the catalyst bed, only liquid-to-particle mass transfer $(k_{Ls}a_s)_{TB}$ and $k\eta$ determine the amount of reaction. In the differential reactor the conversion of isobutene in the liquid feed per pass was 2 to 9%, except at the lowest liquid rate. As shown later for these low conversions, equilibrium between gas and liquid is closely approached throughout the catalyst bed.

Due to pressure drop through the reactor, the pressure of isobutene in the gas entering the reactor was greater than that in the reservoir. To achieve equilibrium for isobutene between the gas and liquid feed streams, the temperature in the reservoir was lowered 1 to 3 K below that at the top of the reactor. For these runs a preheater was used to heat the liquid to the reactor temperature.

Calculation of reaction rates

In trickle-bed operation, TBA is stripped from the reactor by the gas stream as well as in the reservoir. Hence the expression analogous to Eq. 1 is

$$V_T\left(\frac{dC_A}{dt}\right)_{rx} = rm - \left(\begin{matrix}\text{total rate of}\\ \text{TBA loss}\end{matrix}\right) \tag{7}$$

The total TBA loss was found experimentally, as before, from blank runs. These runs were made by adding TBA to the liquid and replacing the catalyst particles with glass beads. All other conditions were the same as for the reaction runs. The TBA loss was found to depend on the gas rate through the trickle bed but was independent of the liquid rate. At gas flow rates of 1.7×10^{-6} and 5.5×10^{-6} m^3/s and a temperature of 323 K, the evaporation was 8.7 and 18.5%, respectively, of the TBA accumulation rate in the reservoir.

Trickle-bed reaction rates

Figure 7 shows reaction rates calculated from Eq. 7 and the measured change in C_A with time. Also, liquid-full rates for the same conditions are included. The latter values increase with liquid rate and approach the asymptotic result of 4.4×10^{-7} kmol/kg · s at $Q_L = \infty$ as determined earlier. The decrease in reaction rate at low Q_L is due to decreasing $(k_{Ls}a_s)_{Lf}$ as the velocity decreases.

The difference between the two curves at intermediate liquid rates is due to the smaller liquid-to-particle mass transfer rate in trickle-bed operation. Because of the pressure drop in the trickle bed, the isobutene concentration, C_L^*, in the feed is up to 3% higher than in the liquid-full runs. At the same concentration the trickle-bed curve would differ slightly more from the liquid-full curve.

The trickle-bed curve exhibits a maximum near the highest liquid rate. We believe this to be due to a shift into the dispersed bubble flow from the trickling-flow regime. Visual observation showed some foaming at the highest liquid rate. Also, the flow regime diagrams of Tosun (1984) and of Charpentier and Favier (1975) indicate that at the highest liquid rate conditions are inside the dispersed bubble flow regime.

Most of the trickle-bed data were obtained at a gas rate of 1.7×10^{-6} m^3/s but one run was made at a threefold higher Q_g. As shown in Figure 7 the reaction rate was essentially unchanged. This is not unexpected since mass transfer rates from gas to liquid for slightly soluble components such as isobutene are not sensitive to gas flow rates. The equality of the reaction rates at different Q_g is also consistent with the conclusion that the gas and liquid remain at near equilibrium throughout the catalyst bed. However, this equilibrium is due to the low con-

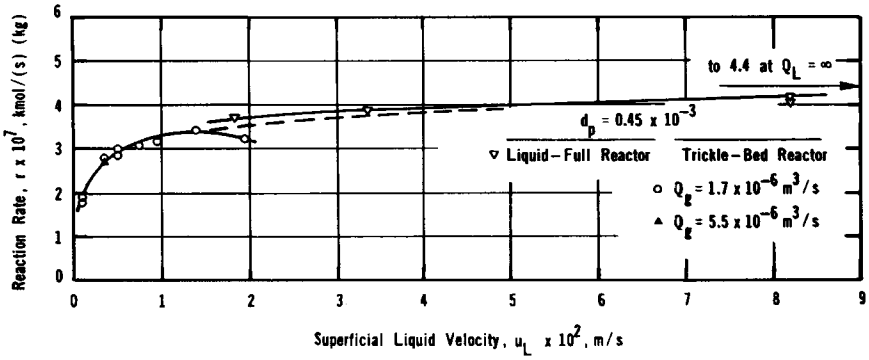

Figure 7. Trickle-bed and liquid-full reaction rates at 323 K for A-15D catalyst.

version per pass and can be shown by estimating the ratio of the isobutene concentration in the liquid effluent to that in the liquid feed. This ratio may be expressed as

$$\frac{C_{L,e}}{C_L^*} = \frac{(k_{gL}a_L) + (1 - x_B)\dfrac{2\,Q_L}{m}}{\dfrac{2\,Q_L}{m} + k_{gL}a_L} \tag{8}$$

where x_B is the conversion per pass. Using the correlation of Fukushima and Kusaka (1977) for $k_{gL}a_L$ in trickle beds, the average concentration ratio, $(C_L)_{av}/C_L^*$ is estimated to range from 0.93 to 0.98, indicating close to equilibrium conditions.

Liquid-to-particle mass transfer coefficients (trickle bed)

Since the trickle-bed rates are dependent only on $k\eta$ and $(k_{Ls}a_s)_{TB}$,

$$r = k\eta C_s = (k_{Ls}a_s)_{TB}[(C_L)_{av} - C_s] \tag{9}$$

With Eq. 8 for $C_{L,e}$, $(C_L)_{av}$ may be expressed as

$$(C_L)_{av} = \frac{C_{L,e} + C_L^*}{2} = \frac{C_L^*}{2} \cdot \left[1 + \frac{(k_{gL}a_L) + (1 - x_B)\left(\dfrac{2\,Q_L}{m}\right)}{k_{gL}a_L + \dfrac{2\,Q_L}{m}}\right] \tag{10}$$

With $k_{gL}a_L$ taken from the correlation of Fukushima and Kusaka, $(k_{gL}a_L)$ is only 0.3 to 4% of $2\,Q_L/m$. Neglecting $k_{gL}a_L$ in evaluating $(C_L)_{av}$ from Eq. 10, and eliminating C_s from Eq. 9, the rate is given by

$$r = \frac{\left(1 - \dfrac{x_B}{2}\right)C_L^*}{1/k\eta + 1/(k_{Ls}a_s)_{TB}} \tag{11}$$

The conversion per pass is related to the rate by

$$x_B = \frac{mr}{Q_L C_L^*} \tag{12}$$

Eliminating x_B from Eq. 11 with Eq. 12 and solving for $(k_{Ls}a_s)_{TB}$ yields

$$(k_{Ls}a_s)_{TB} = \left(\frac{C_L^*}{r} - \frac{1}{k\eta} - \frac{m}{2\,Q_L}\right)^{-1} \tag{13}$$

Equation 13 gives $(k_{Ls}a_s)_{TB}$ in terms of $k\eta$ determined from the liquid-full experiments and quantities measured in the trickle-bed runs. That C_L^* was indeed the solubility of isobutene in the reservoir was tested by analyzing the liquid feed concentration at the maximum Q_L. The results were within 3% of the solubilities shown in Table 5.

Equations 9 and 11 are applicable only for a wetting efficiency f of unity. The correlations of Satterfield (1975) and Herskowitz and Smith (1983) indicate that f is well above 0.90 at all liquid flow rates except for our lowest value. Hence, $(k_{Ls}a_s)_{TB}$ can be calculated for all our liquid flow rates except the lowest and the highest, where a change in flow regime seems likely. Results are given in Figure 8, where the values from Eq. 13 are plotted along with the correlations of Goto and Smith (1975) and Dharwadkar and Sylvester (1977).

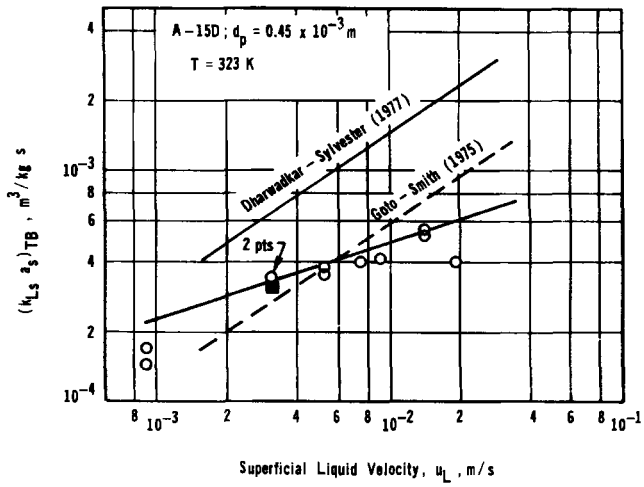

Figure 8. Liquid-to-particle mass transfer coefficients in trickle-bed operation.

The correlations shown in Figure 8 are based upon dissolution data where mass transfer was the direct result of the experiments. Since the dissolving particles were nonporous, a_s was taken as $a_t\,\epsilon_p$ to be comparable with our $(k_{Ls}a_s)_{TB}$ values. The results agree approximately with the earlier Goto and Smith correlation but are lower than the Dharwadkar and Sylvester values.

It is important to note that in the trickle-bed experiments an average of about 20% of the total resistance (Eq. 13) for the global rate was due to liquid-to-particle mass transfer. Hence, the $(k_{Ls}a_s)_{TB}$ results in Figure 8 are not particularly accurate. In contrast, the $k\eta$ results from liquid-full experiments should be of good accuracy since mass transfer contributed only 4 to 11% (for the 0.45×10^{-3} m particles) of the total resistance over the range of liquid flow rates studied.

For a reactant in the gas phase the effect of wetting efficiencies less than 100% is to increase the global reaction rate. Whether this effect is significant depends upon the importance of liquid-to-particle mass transfer. In our case where this mass transfer resistance was only 20% of the total, an increase in rate at low Q_L, where $f < 100\%$, was not observed (Figure 7). Since the liquid and gas phase were in near equilibrium, the low mass transfer resistance means that the isobutene concentration was about the same on liquid-covered as on gas-covered outer surface of the particles. At these conditions the wetting efficiency does not affect the rate. For a much more active catalyst the trickle-bed curve in Figure 7 would be expected to show a minimum and turn toward higher reaction rates at low liquid flow rates.

Acknowledgment

Grants from the U.S.-Spain Committee for Scientific and Technological Cooperation (to F. Recasens) and from CIRIT, Generalitat de Catalunya (to C. Zorrilla) are gratefully acknowledged. We thank the Rohm and Haas Co. for providing the catalysts.

Notation

a_L = gas-to-liquid mass transfer area, m^2/kg catalyst
a_s = liquid-to-particle mass transfer area, m^2/kg catalyst
a_t = external area of particle, m^2/kg
$\bar{a}_r$ = average pore diameter, m
C_A = TBA concentration in liquid, kmol/m^3
C_g = isobutene concentration in gas, kmol/m^3
C_L = isobutene concentration in bulk liquid, kmol/m^3
C_{Le} = concentration in effluent from catalyst bed
C_L^* = concentration in liquid in equilibrium with C_g
C_s = concentration at external surface of catalyst particle
D = diffusivity of isobutene, m^2/s
D_e = effective intraparticle diffusivity of isobutene, m^2/s
d_p = diameter of spherical catalyst particle, m
f = fraction of external surface of catalyst particle covered by liquid
H_A = Henry's law coefficient for TBA in water, $(C_A)_g/C_A$
H = Henry's law coefficient for isobutene in water, C_g/C_L
k = first-order intrinsic rate constant, m^3/s · kg dry catalyst
k_{gL} = gas-to-liquid mass transfer coefficient, m/s
$(k_{Ls}a_s)_{Lf}$ = liquid-to-particle mass transfer coefficient in liquid-full operation, m^3/kg catalyst · s
$(k_{Ls}a_s)_{TB}$ = liquid-to-particle mass transfer coefficient in trickle-bed operation, m^3/kg catalyst · s
m = mass of dry catalyst, kg
Q_g, Q_L = volumetric flow rates of gas or liquid, m^3/s
r = rate of production of TBA, kmol/s · kg dry catalyst
t = time, s
T = temperature, K
u_g, u_L = superficial velocities of gas and liquid incatalyst bed, m/s
V_g = cumulative pore volume at 4.13 MPa, m^3/kg
V_T = total liquid volume in system, m^3

Greek letters

α = proportionality constant in Eq. 1
ϵ_p = porosity of catalyst particles
η = effectiveness factor
μ_L = viscosity of liquid, kg/m · s
ρ_c = catalyst solid density, kg dry solid/m^3
ρ_L = density of liquid, kg/m^3
ρ_p = catalyst particle density, kg dry particle/vol. wet particle
ϕ = Thiele modulus,

Literature cited

Charpentier, J. C., and M. Favier, "Some Liquid Holdup Experimental Data in Trickle-Bed Reactors for Foaming and Nonfoaming Hydrocarbons," *AIChE J.*, **21**, 1213 (1975).

Dharwadkar, A., and N. D. Sylvester, "Liquid-Solid Mass Transfer in Trickle Beds," *AIChE J.*, **23**, 376 (1977).

Dooley, K. M., J. A. Williams, B. C. Gates, and R. L. Albright, "Sulfonated Poly (styrene divinylbenzene) Catalysts," *J. Catalysis*, **74**, 361 (1982).

Dwivedi, P. N., and S. N. Upadhyay, "Particle-Fluid Mass Transfer in Fixed and Fluidized Beds," *Ind. Eng. Chem., Proc. Des. Dev.*, **16**, 157 (1977).

Fukushima, S., and K. Kusaka, "Liquid-Phase Volumetric Mass-Transfer Coefficients and Boundary of Hydrodynamics Flow Region in Packed Column with Cocurrent Downward Flow," *J. Chem. Eng. Japan*, **10**, 468 (1977).

Gates, B. C., and W. Rodriguez, "General and Specific Acid Catalysis in Sulfonic Acid Resin," *J. Catalysis*, **31**, 27 (1973).

Gehlawat, J. K., and M. M. Sharma, "Absorption of Isobutylene in Aqueous Solutions of Sulfuric Acid," *Chem. Eng. Sci.*, **23**, 1173 (1968).

Goto, S., and J. M. Smith, "Trickle-Bed Reactor Performance," *AIChE J.*, **21**, 707 (1975).

Gupta, V. P., and W. J. M. Douglas, "Diffusion and Chemical Reaction in Isobutene Hydration within Cation Exchange Resin," *AIChE J.*, **13**, 883 (1967).

Heath, H. W., Jr., and B. C. Gates, "Mass Transport and Reaction in Sulfonic Acid Resin Catalyst: The Dehyration of t-Butyl Alcohol," *AIChE J.*, **18**, 321 (1972).

Herskowitz, M., and J. M. Smith, "Liquid Distribution in Trickle-Bed Reactors," *AIChE J.*, **24**, 439 (1978).

———, "Trickle-Bed Reactors: A Review," *AIChE J.*, **29**, 1 (1983).

Herskowitz, M., R. G. Carbonell, and J. M. Smith, "Effectiveness Factors and Mass Transfer in Trickle-Bed Reactors," *AIChE J.*, **25**, 272 (1979).

Ihn, S.-K., and I.-H. Oh, "Correlation of a Two-Phase Model for Macroreticular Resin Catalyst in Sucrose Inversion," *J. Chem. Eng. Japan*, **17**, 58 (1984).

Kaiser, J. R., H. Beuther, L. D. Moore, and R. C. Odioso, "Direct Hydration of Propylene over Ion-exchange Resins," *Ind. Eng. Chem., Prod. Res. Dev.*, **1**, 296 (1962).

Kazanskii, K. S., S. G. Entelis, and N. M. Chirkov, "Solubility of Gaseous Isobutylene in Water," *Z. Fiz, Khim.*, **23**, 1409 (1959).

Kun, K. A., and R. Kunin, "The Pore Structure of Macroreticular Ion-exchange Resins," *J. Poly. Sci. Part C*, **16**, 1457 (1967).

Lucas, H. S., and W. F. Eberz, "The Hydration of Unsaturated Compounds," *J. Am. Chem. Soc.*, **56**, 460 (1934).

Morita, Shushi, and J. M. Smith, "Mass Transfer and Contacting Efficiency in a Trickle-Bed Reactor," *Ind. and Eng. Chem. Fundamentals*, **17**, 113 (1978).

Neier, W., and J. Woellner, "Isopropyl Alcohol by Direct Hydration," *Chem. Tech.*, p. 95 (Feb., 1973).

O'Sullivan, D. A., "ARCO Increasing Stake in Western Europe," *Chem. Eng. News.*, p. 70 (Mar. 18, 1985).

Pitochelli, A. R., "Ion-exchange Catalysis and Matrix Effects," Technical Bulletin, Rohm and Haas Co., Philadelphia (1975).

Satterfield, C. N., *Mass Transfer in Heterogeneous Catalysis*, MIT, Cambridge, MA (1970).

———, "Trickle-Bed Reactors," *AIChE J.*, **21**, 209 (1975).

Smith, J. M., *Chemical Engineering Kinetics*, 3rd ed., McGraw-Hill New York, 486 (1981).

Taft, R. W., E. L. Purlee, and P. Riesz, "A Method for Determining the Distribution Constant for a Substance between the Gas Phase and a Condensed Phase," *J. Am. Chem. Soc.*, **77**, 899 (1955).

Tosun, G. "A Study of Downflow of Nonfoaming Gas-Liquid Systems in a Packed Bed. 1: Flow Regimens: Search for a Generalized Flow Map," *Ind. Eng. Chem.*, **23**, 29 (1984).

Manuscript received Dec. 30, 1985, and revision received Feb. 21, 1986.